

Progressive Skeletonization: Trimming more fat from a network at initialization

Pau de Jorge^{*,1}, Amartya Sanyal², Harkirat S. Behl²,
Philip H.S. Torr², Gregory Rogez¹, and Puneet K. Dokania^{2,3}

¹NAVER LABS Europe, Grenoble, France[†]

²University of Oxford, UK

³Five AI Ltd., UK

Abstract

Recent studies have shown that skeletonization (pruning parameters) of networks *at initialization* provides all the practical benefits of sparsity both at inference and training time, while only marginally degrading their performance. However, we observe that beyond a certain level of sparsity (approx 95%), these approaches fail to preserve the network performance, and to our surprise, in many cases perform even worse than trivial random pruning. To this end, we propose to find a skeletonized network with maximum *foresight connection sensitivity* (FORCE). Intuitively, out of all possible sub-networks, we propose to find the one whose connections would have a maximum impact on the loss when perturbed. Our approximate solution to maximize the FORCE, progressively prunes connections of a given network at initialization. This allows parameters that were unimportant at earlier stages of skeletonization to become important at later stages. In many cases, our approach enables us to remove up to 99.9% parameters, while keeping networks trainable and providing significantly better performance than recent approaches. We demonstrate the effectiveness of our approach at various levels of sparsity (from medium to extreme) through extensive experiments and analysis.

1 Introduction

The majority of pruning algorithms for Deep Neural Networks require training the dense models and often fine-tuning sparse sub-networks in order to obtain their pruned counterparts. In Frankle and Carbin [2019], the authors provide empirical evidence that there exist sparse sub-networks that can be trained from scratch to achieve similar performance as their dense counterparts. However, their method to find such sub-networks requires training the full-sized model and intermediate sub-networks, making the process much more expensive.

Recently, Lee et al. [2019] presented SNIP. Building upon a three decades old saliency criterion for pruning trained models (Mozer and Smolensky [1989]), they are able to predict, at initialization, the importance each weight will have later in training. Pruning at initialization methods are much cheaper than conventional pruning methods. Moreover, while traditional pruning methods can help accelerate inference tasks Elsen et al. [2019], pruning at initialization may go one step further and provide the same benefits at train time.

Wang et al. [2020] (GRASP) noted that after applying the pruning mask, gradients will be modified due to non-trivial interactions between weights. Thus, maximizing SNIP criterion before pruning is sub-optimal, as it assumes that the effect of removing each weight is independent, which might not be true. Moreover, they state that at initialization, the loss might not be informative and choose to preserve the gradient norm *after*

^{*}Work done while being a visitor at University of Oxford. Correspondence to pau@robots.ox.ac.uk

[†]Please visit www.europe.naverlabs.com

pruning. To approximate the gradient norm after pruning, the authors treat pruning as a perturbation on the weight matrix and use the first order Taylor’s approximation.

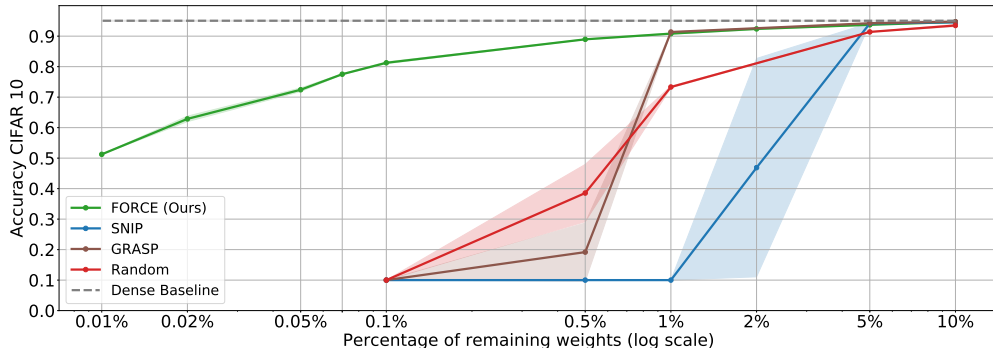


Figure 1: Test accuracies on CIFAR-10 (ResNet50) for different pruning methods. Each point is the average over 3 runs of prune-train-test. The shaded areas denote the standard deviation of the runs (too small to be visible in some cases). Random corresponds to removing connections uniformly.

We argue that both the SNIP and GRASP approximations of the gradients after pruning are not valid for high levels of sparsity, where a large portion of the weights are removed simultaneously. In this work, we go back to the criteria introduced by Mozer and Smolensky [1989], but we optimize what this saliency would be *after* pruning, rather than *before*. Hence, we name our criteria *Foresight Connection sEnsitivity* (FORCE). Moreover, both SNIP and GRASP are one-shot approximations, removing all the weights at once. We introduce an algorithm that progressively skeletonizes the network, removing a small fraction of weights at each step and re-computing the gradients after each pruning round. This allows to take into account the intricate interactions between weights, re-adjusting the importance of connections at each step. We show that SNIP can be viewed as an approximation of our method (FORCE). Empirically, we find that both SNIP and GRASP have a sharp drop in performance when targeting higher levels of sparsity. Surprisingly, they perform even worse than random pruning as can be seen in Figure 1. In contrast, our proposed pruning scheme enables pruning at extreme sparsity levels on a wide range of datasets.

2 Related work

Pruning trained models Most of the pruning works follow the *train – prune – fine-tune* cycle (Mozer and Smolensky [1989], LeCun et al. [1990], Hassibi et al. [1993], Han et al. [2015], Molchanov et al. [2017], Guo et al. [2016]), which requires training the dense network until convergence, followed by multiple iterations of pruning and fine-tuning until a target sparsity is reached. Frankle and Carbin [2019] showed that it was possible to find sparse sub-networks that, when trained from scratch, were able to match or even surpass the performance of their dense counterparts. Nevertheless, to find them they use a costly procedure based on Han et al. [2015]. All these methods rely on having a trained network, thus, they are not applicable before training. In contrast, our algorithm is able to find a trainable sub-network with randomly initialized weights. Making the overall pruning cost much cheaper and presenting an opportunity to leverage the sparsity during training as well.

Induce sparsity during training Another popular approach has been to induce sparsity during training. This can be achieved by modifying the loss function to consider sparsity as part of the optimization (Chauvin [1989], Carreira-Perpiñán and Idelbayev [2018], Louizos et al. [2018]) or by dynamically pruning during training (Bellec et al. [2018], Mocanu et al. [2018], Mostafa and Wang [2019], Dai et al. [2019], Dettmers and Zettlemoyer [2020], Lin et al. [2020], Kusupati et al. [2020]). Although these methods are cheaper than pruning after training, they need at least the same computational effort as training a dense network to find

the sparse sub-network. Moreover, they usually need a fine-tuning round to fully optimize the final sparse model. Our method is able to prune the network before starting the training, thus, we do not require any additional memory and computation. Since we do all the training with the sparse sub-network from scratch, we do not require any additional fine-tuning either.

Pruning at initialization These methods present a significant leap with respect to other pruning methods. While traditional pruning mechanisms can only be used to bring speed-up and memory reduction at inference time, pruning at initialization brings the same gains both at training and inference time. This can only be achieved when pruning before training. Lee et al. [2019] presented SNIP, a method to estimate, at initialization, the importance that each weight could have later during training. SNIP analyses the effect of each weight on the loss function when perturbed at initialization. In Lee et al. [2020] the authors perform a theoretical study of pruning at initialization from a signal propagation perspective, focusing on the initialization scheme. Recently, Wang et al. [2020] proposed GRASP, a different method based on the gradient norm after pruning and showed a significant improvement for moderate levels of sparsity. However, neither SNIP nor GRASP perform sufficiently well when larger compressions and speed-ups are required and a larger fraction of the weights need to be pruned. In this paper, we analyse the approximations made by SNIP and GRASP and present a more suitable solution to maximize the saliency after pruning.

3 Problem Formulation: Pruning at Initialization

Given a dataset $\mathcal{D} = \{(\mathbf{x}_i, \mathbf{y}_i)\}_{i=1}^n$, the training of a neural network f parameterized by $\boldsymbol{\theta} \in \mathbb{R}^m$ can be written as minimizing the following empirical risk:

$$\arg \min_{\boldsymbol{\theta}} \frac{1}{n} \sum_i \mathcal{L}((f(\mathbf{x}_i; \boldsymbol{\theta})), \mathbf{y}_i) \quad \text{s.t. } \boldsymbol{\theta} \in \mathcal{C}, \quad (1)$$

where \mathcal{L} and \mathcal{C} denote the loss function and the constraint set respectively. Unconstrained (standard) training corresponds to $\mathcal{C} = \mathbb{R}^m$. Assuming we have access to the gradients (batch-wise) of the empirical risk, an optimization algorithm (*e.g.* SGD) is generally used to optimize the above objective, that, during the optimization process, produces a sequence of iterates $\{\boldsymbol{\theta}_i\}_{i=0}^T$, where $\boldsymbol{\theta}_0$ and $\boldsymbol{\theta}_T$ denote the initial and the final (optimal) parameters, respectively. Given a target sparsity level of $k < m$, the *general* parameter pruning problem involves \mathcal{C} with a constraint $\|\boldsymbol{\theta}_T\|_0 \leq k$, *i.e.*, the final optimal iterate must have a maximum of k non-zero elements. Note that there is no such constraint with the intermediate iterates.

Pruning at initialization, the main focus of this work, adds further restrictions to the above mentioned formulation by constraining all the iterates to lie in a *fixed* subspace of \mathcal{C} . Precisely, the constraints are to find a $\boldsymbol{\theta}_0$ such that $\|\boldsymbol{\theta}_0\|_0 \leq k$ ¹, and the intermediate iterates $\boldsymbol{\theta}_i \in \bar{\mathcal{C}} \subset \mathcal{C}$, $\forall i \in \{1, \dots, T\}$, where $\bar{\mathcal{C}}$ is the subspace of \mathbb{R}^m spanned by the natural basis vectors $\{\mathbf{e}_j\}_{j \in \text{supp}(\boldsymbol{\theta}_0)}$. Here, $\text{supp}(\boldsymbol{\theta}_0)$ denotes the support of $\boldsymbol{\theta}_0$, *i.e.*, the set of indices with non-zero entries. The first condition defines the sub-network at initialization with k parameters, and the second fixes its topology throughout the training process. Since there are $\binom{m}{k}$ such possible sub-spaces, exhaustive search to find the optimal sub-space to maximize (1) is impractical as it would require training a neural network $\binom{m}{k}$ times. Below we discuss two recent approaches that circumvent this problem by maximizing a hand-designed data-dependent objective function. These objective functions are tailored to preserve some relationships between the parameters, the loss, and the dataset, that *might* be sufficient to obtain a reliable $\boldsymbol{\theta}_0$. For ease of notation, we will use $\boldsymbol{\theta}$ to denote the value of the dense initialization.

SNIP Lee et al. [2019] present a method based on the saliency criterion from Mozer and Smolensky [1989]. They add a key insight and show this criteria works surprisingly well to predict, at initialization, the importance each connection will have during training. The idea is to preserve the parameters that will have

¹In practice, as will be done in this work as well, a subset of a *given* dense initialization is found using some saliency criterion (will be discussed soon), however, note that our problem statement is more general than that.

maximum impact on the loss when perturbed. Let $\mathbf{c} \in \{0, 1\}^m$ be a binary vector, and \odot the Hadamard product. Then, the *connection sensitivity* in SNIP is computed as:

$$\mathbf{g}(\boldsymbol{\theta}) := \left. \frac{\partial \mathcal{L}(\boldsymbol{\theta} \odot \mathbf{c})}{\partial \mathbf{c}} \right|_{\mathbf{c}=\mathbf{1}} = \frac{\partial \mathcal{L}(\boldsymbol{\theta})}{\partial \boldsymbol{\theta}} \odot \boldsymbol{\theta}. \quad (2)$$

Once $\mathbf{g}(\boldsymbol{\theta})$ is obtained, the parameters corresponding to the top- k values of $|\mathbf{g}(\boldsymbol{\theta})_i|$ are then kept. Intuitively, SNIP favors those weights that are far from the origin *and* provide high gradients (irrespective of the direction). We note that SNIP objective can be written as the following problem:

$$\max_{\mathbf{c}} S(\boldsymbol{\theta}, \mathbf{c}) := \sum_{i \in \text{supp}(\mathbf{c})} |\theta_i \nabla \mathcal{L}(\boldsymbol{\theta})_i| \quad \text{s.t. } \mathbf{c} \in \{0, 1\}^m, \|\mathbf{c}\|_0 = k. \quad (3)$$

It is trivial to note that the optimal solution to the above problem can be obtained by selecting the indices corresponding to the top- k values of $|\theta_i \nabla \mathcal{L}(\boldsymbol{\theta})_i|$.

GRASP Wang et al. [2020] note that the SNIP saliency is measuring the *connection sensitivity* of the weights *before* pruning, however, it is likely to change after pruning. Moreover, they argue that, at initialization, it is more important to preserve the gradient signal than the loss itself. They propose to use as saliency the gradient norm of the loss $\Delta \mathcal{L}(\boldsymbol{\theta}) = \nabla \mathcal{L}(\boldsymbol{\theta})^T \nabla \mathcal{L}(\boldsymbol{\theta})$, but measured *after* pruning. To maximize it, Wang et al. [2020] adopt the same approximation introduced in LeCun et al. [1990] and treat pruning as a perturbation on the initial weights. Their method is equivalent to solving:

$$\max_{\mathbf{c}} G(\boldsymbol{\theta}, \mathbf{c}) := \sum_{\{i: c_i=0\}} -\theta_i [\mathbf{H}\mathbf{g}]_i \quad \text{s.t. } \mathbf{c} \in \{0, 1\}^m, \|\mathbf{c}\|_0 = k. \quad (4)$$

Where \mathbf{H} and \mathbf{g} denote the Hessian and the gradient of the loss respectively.

4 Foresight Connection Sensitivity

Since removing weights from a network will have a strong influence on the gradients, we are interested in finding the *connection sensitivity* of the loss function *after* pruning, which we name *Foresight Connection Sensitivity* (FORCE). We argue this will provide a better indication of the training dynamics of the pruned network. Let $\bar{\boldsymbol{\theta}} = \boldsymbol{\theta} \odot \mathbf{c}$ denote the pruned parameters after a binary mask \mathbf{c} with $\|\mathbf{c}\|_0 = k < m$ is applied. The FORCE at $\bar{\boldsymbol{\theta}}$ for a given mask $\hat{\mathbf{c}}$ is obtained as follows:

$$\mathbf{g}(\bar{\boldsymbol{\theta}}) := \left. \frac{\partial \mathcal{L}(\bar{\boldsymbol{\theta}})}{\partial \mathbf{c}} \right|_{\mathbf{c}=\hat{\mathbf{c}}} = \left. \frac{\partial \mathcal{L}(\bar{\boldsymbol{\theta}})}{\partial \bar{\boldsymbol{\theta}}} \right|_{\mathbf{c}=\hat{\mathbf{c}}} \odot \left. \frac{\partial \bar{\boldsymbol{\theta}}}{\partial \mathbf{c}} \right|_{\mathbf{c}=\hat{\mathbf{c}}} = \left. \frac{\partial \mathcal{L}(\bar{\boldsymbol{\theta}})}{\partial \bar{\boldsymbol{\theta}}} \right|_{\mathbf{c}=\hat{\mathbf{c}}} \odot \boldsymbol{\theta}. \quad (5)$$

The last equality is obtained by rewriting $\bar{\boldsymbol{\theta}}$ as $\text{diag}(\boldsymbol{\theta})\mathbf{c}$, where $\text{diag}(\boldsymbol{\theta})$ is a diagonal matrix with $\boldsymbol{\theta}$ as its elements, and then differentiating w.r.t. \mathbf{c} . We now discuss the crucial differences between our formulation (5), SNIP (2) and GRASP (4).

- When $\hat{\mathbf{c}} = \mathbf{1}$, the formulation is exactly the same as the connection sensitivity used in SNIP. However, $\hat{\mathbf{c}} = \mathbf{1}$ is too restrictive in the sense that it assumes that all the parameters are active in the network and they are removed one by one *with replacement*, therefore, it fails to capture the impact of removing a group of parameters.
- Our formulation, similar to Wang et al. [2020], is based on the gradients at the pruned set of parameters $\bar{\boldsymbol{\theta}}$, thus, they provide a better indication of the training dynamics than SNIP. However, GRASP formulation is based on the assumption that pruning is a small perturbation on the Gradient Norm which is not reasonable for high sparsity levels.

- In the case of extreme pruning, *i.e.*, when $\|\hat{\mathbf{c}}\|_0 \ll \|\mathbf{1}\|_0 = m$, the gradients before and after pruning will have very different values as $\|\boldsymbol{\theta} \odot \hat{\mathbf{c}}\|_2 \ll \|\boldsymbol{\theta}\|_2$, thus, making SNIP and GRASP unreliable (empirically we find SNIP and GRASP fail in the case of extreme pruning).

FORCE saliency Note FORCE (5) is defined for a given sub-network which is unknown *a priori*, as our objective itself is to find the sub-network with maximum connection sensitivity. Similar to the reformulation of SNIP in (3), the objective to find such sub-network corresponding to the foresight connection sensitivity can be written as:

$$\max_{\mathbf{c}} S(\boldsymbol{\theta}, \mathbf{c}) := \sum_{i \in \text{supp}(\mathbf{c})} |\theta_i \nabla \mathcal{L}(\boldsymbol{\theta} \odot \mathbf{c})_i| \quad \text{s.t. } \mathbf{c} \in \{0, 1\}^m, \|\mathbf{c}\|_0 = k. \quad (6)$$

Here $\nabla \mathcal{L}(\boldsymbol{\theta} \odot \mathbf{c})_i$ represents the i -th index of $\left. \frac{\partial \mathcal{L}(\bar{\boldsymbol{\theta}})}{\partial \boldsymbol{\theta}} \right|_{\mathbf{c}}$. As opposed to (3), finding the optimal solution of (6) is non trivial as it requires computing the gradients of all possible $\binom{m}{k}$ sub-networks in order to find the one with maximum sensitivity. To this end, below, we propose an approximate solution to the above problem that primarily involves (i) progressively increasing the degree of pruning, and (ii) solving problem (3) at each stage of pruning.

Progressive skeletonization Let k be the number of parameters to be kept after pruning. Let us assume that we know a schedule (will be discussed later) to divide k into a set of natural numbers $\{k_t\}_{t=1}^T$ such that $k_t > k_{t+1}$ and $k_T = k$. Now, given the mask \mathbf{c}_t corresponding to k_t , pruning from k_t to k_{t+1} can be formulated using the connection sensitivity (5) as:

$$\mathbf{c}_{t+1} = \arg \max_{\mathbf{c}} S(\bar{\boldsymbol{\theta}}, \mathbf{c}) \quad \text{s.t. } \mathbf{c} \in \{0, 1\}^m, \|\mathbf{c}\|_0 = k_{t+1}, \mathbf{c} \odot \mathbf{c}_t = \mathbf{c}, \quad (7)$$

where $\bar{\boldsymbol{\theta}} = \boldsymbol{\theta} \odot \mathbf{c}_t$. The constraint $\mathbf{c} \odot \mathbf{c}_t = \mathbf{c}$ ensures that no parameter that had been pruned earlier is activated again. Assuming that the pruning schedule ensures a smooth transition from one topology to another ($\|\mathbf{c}_t\|_0 \approx \|\mathbf{c}_{t+1}\|_0$) such that the *gradient approximation* $\left. \frac{\partial \mathcal{L}(\bar{\boldsymbol{\theta}})}{\partial \boldsymbol{\theta}} \right|_{\mathbf{c}_t} \approx \left. \frac{\partial \mathcal{L}(\bar{\boldsymbol{\theta}})}{\partial \boldsymbol{\theta}} \right|_{\mathbf{c}_{t+1}}$ is valid, (7) can be approximated as solving (3) at $\bar{\boldsymbol{\theta}}$. Thus, for a given schedule over k , our approximate solution to (6) involves solving (3) iteratively. That would finally lead to a sub-network with k non-zero parameters. An overview of the method can be found in Algorithm 1. An important property of this approach is that once a parameter has been pruned at iteration t , its impact on the loss function and the gradient computation is nil for the remaining pruning iterations. Conversely, a parameter or connection that is not important at t , might become important at the following iterations depending on the sub-network obtained at t as the loss and the gradients are computed on the sub-network, not the entire network we started with. Note, for a schedule with $T = 1$, we recover SNIP. Thus, SNIP can be seen as an instance of our method where we use the *gradient approximation* between the dense network, $\mathbf{c}_0 = \mathbf{1}$ and the final mask \mathbf{c} .

Sparsity schedule In order to choose $\{k_t\}_{t=1}^T$, we conduct an ablation study of the effect of different values for T , see Figure 4. Moreover, we suggest two different approaches for the evolution of sparsity levels. In the first scenario, k_t simply follows a linear decay between m and k . As we increase the sparsity level, the last iterations will need to compute $S(\boldsymbol{\theta} \odot \mathbf{c}_t, \mathbf{c}_{t+1})$ where $\|\mathbf{c}_t\|_0 = k_t$ is already quite low. This means that the *gradient approximation* might no longer hold, since the amount of weights to be removed versus the amount of remaining weights is not negligible. This motivates our second proposal where k_t decays exponentially, eliminating more weights in the first iterations and then gradually removing less weights as the network is further pruned. More formally:

$$\text{Linear mode: } k_t = \alpha k + (1 - \alpha)m, \quad \alpha = \frac{t}{T} \quad (8)$$

$$\text{Exp mode: } k_t = \exp \{ \alpha \log k + (1 - \alpha) \log m \}, \quad \alpha = \frac{t}{T}. \quad (9)$$

Some theoretical insights Intuitively, when pruning weights gradually, we are looking for the best possible sub-network in a neighbourhood defined by the previous mask and the amount of weights removed at that step.

The problem being non-convex and non-smooth makes it challenging to prove whether the mask obtained by our method is globally optimal or not. However, in Appendix C we prove that each iterative mask obtained with gradual pruning is indeed an approximate local minima, where the degree of sub-optimality increases with the pruning step size. This also gives some intuition of why SNIP fails in case of extreme pruning.

Algorithm 1 FORCE algorithm to find a pruning mask

- 1: **Inputs:** Training set \mathcal{D} , final sparsity k , number of steps T , weights $\theta_0 \in \mathbb{R}^m$.
 - 2: Obtain $\{k_t\}_{t=1:T}$ using the chosen schedule (refer to Eq (8) and (9))
 - 3: Define initial mask $c_0 = \mathbf{1}$
 - 4: **for** $t = 0, \dots, T - 1$ **do**
 - 5: Sample mini-batch $\{z_i\}_{i=1}^n$ from \mathcal{D}
 - 6: Define $\bar{\theta} = \theta \odot c_t$
 - 7: Compute $g(\bar{\theta})$ (refer to Eq (5))
 - 8: $I = \{i_1, \dots, i_{k_{t+1}}\}$ are top- k_{t+1} values of $|g_i|$
 - 9: Build c_{t+1} by setting to 0 all indices not included in I .
 - 10: **end for**
 - 11: **Return:** c_T .
-

5 Experiments

We evaluate the efficacy of our approach (FORCE) on CIFAR-10/100 (Krizhevsky et al. [2009]), which consists of 60k 32×32 colour images divided into 10/100 classes, and also on ImageNet (Russakovsky et al. [2015]) and its smaller version Tiny-ImageNet, which respectively consist of 14M/100k and 20k/200 images/classes. Training settings, architecture descriptions, and implementation details are provided in Appendix A.

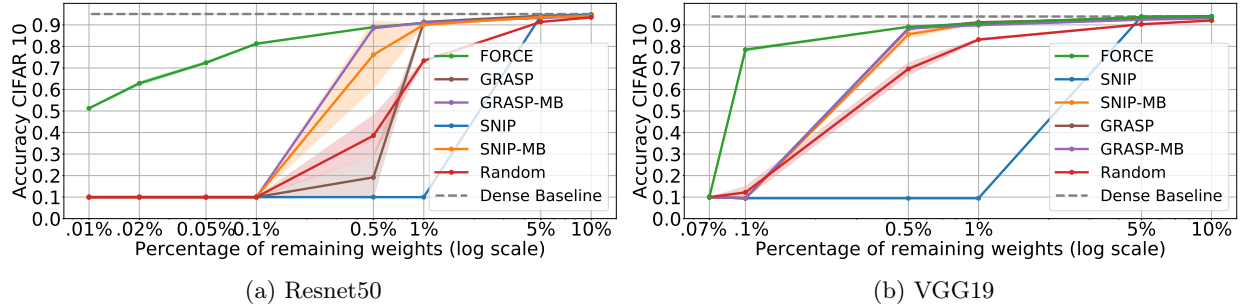


Figure 2: Test accuracies on CIFAR-10 for different pruning methods. When we increase the number of batches (-MB) one-shot methods can prune up to higher sparsity levels, but our gradual pruning method can go even further. Each point is the average over 3 runs of prune-train-test. The shaded areas denote the standard deviation of the runs (too small to be visible in some cases). Note that in (b), GRASP and GRASP-MB overlap.

5.1 Results on CIFAR-10

Figure 2 compares the accuracy of our method with both SNIP and GRASP. We also report the performance of a dense and a random pruning baseline. Both SNIP and GRASP consider a single batch to approximate the saliencies, while we employ a different batch of data at each stage of our gradual skeletonization process. For a fair comparison, and to understand how the number of batches impacts performance, we also run these methods averaging the saliencies over T batches. SNIP-MB and GRASP-MB respectively refer to these

multi-batch (MB) counterparts. In these experiments, we use $T = 300$ and an exponential decay for k_t unless stated otherwise. We analyse the effect of T and decay mode later in Section 5.3.

We observe that for moderate sparsity levels, one batch is sufficient for both SNIP and GRASP as reported in Lee et al. [2019], Wang et al. [2020]. However, as we increase the level of sparsity, the performance of SNIP and GRASP degrades dramatically. For example, at 99.0% sparsity, SNIP based pruned network’s accuracy drops down to 10% for both ResNet50 and VGG19, which is equivalent to random guessing as there are 10 classes. Note, in the case of randomly pruned networks, accuracy is nearly 75% and 82% for ResNet50 and VGG19, respectively, which is significantly better than the performance of SNIP. However, to our surprise, just using multiple batches to compute the connection sensitivity used in SNIP improves it from 10% to 90%. This clearly indicates that a better approximation of the connection sensitivity is necessary for good performance in the case of extreme sparsity regime. Similar trends, although not this extreme, can be observed in the case of GRASP as well. FORCE, clearly outperforms all the above mentioned approaches in all the levels of sparsity. For example, in the case of 99.9% pruning, while all other five approaches perform as good as a random classifier (nearly 10% accuracy), FORCE provides an accuracy of nearly 80%. This is an extremely encouraging result, as, no approach before has pruned a network at initialization to such extremes while providing an acceptable accuracy. These results also indicate the importance of choosing the right pruning criteria, and the approximations used to compute it. As evident, these factors play a crucial role when removing a few extra parameters might change dramatically the topology of a network.

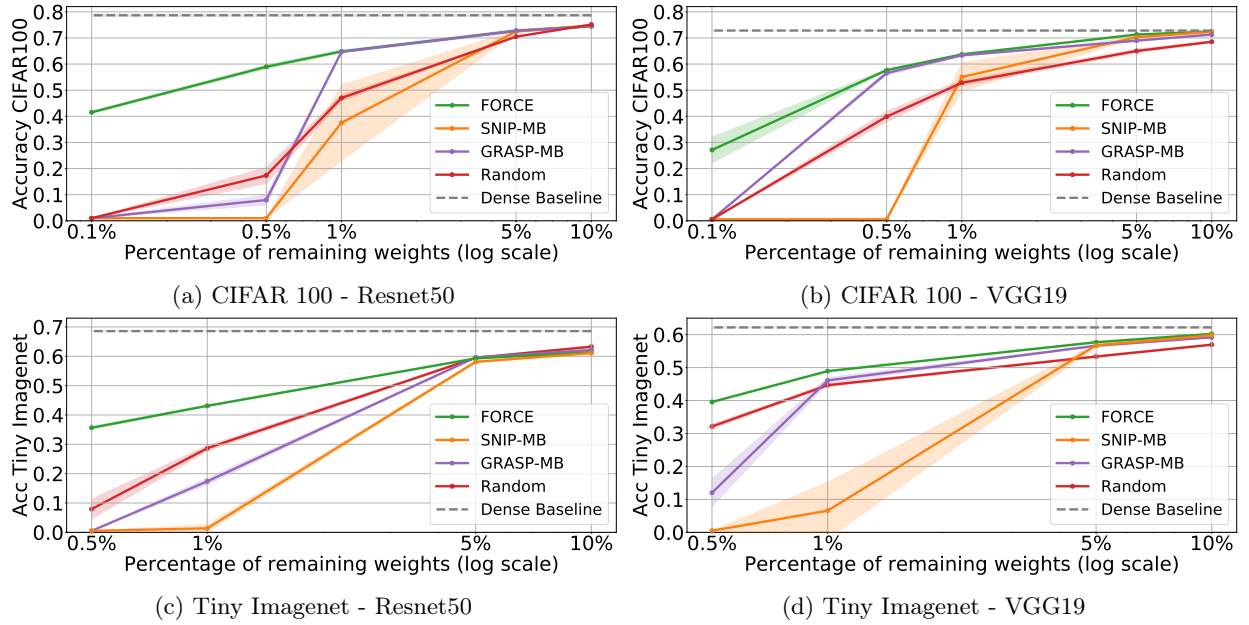


Figure 3: Test accuracies on CIFAR-100 and Tiny Imagenet for different pruning methods. Each point is the average over 3 runs of prune-train-test. The shaded areas denote the standard deviation of the runs (too small to be visible in some cases).

5.2 Results on larger datasets

In this Section, we present experiments on larger, more complex datasets. Wang et al. [2020] and Lee et al. [2019] suggest using a batch of size ~ 10 times the number of classes. Instead of loading a batch with all the examples at once, we average the saliencies over several mini-batches to avoid increasing the memory demand. For CIFAR100 and Tiny-ImageNet, we average 10 and 20 batches per iteration respectively, with 128 examples per batch.

As we increase the number of batches per iteration, computing the pruning mask becomes more expensive. From Figure 4, we observe that both saliency and accuracy converge after just a few iterations. Thus, for the following experiments we used 60 iterations. For a fair comparison, we run SNIP and GRASP with $T \times B$ batches, where T is the number of iterations and B the number of batches per iteration in our method. Results are presented in Figure 3.

In the case of Imagenet, we use a batch size of 256 examples and 40 batches per iteration. We use the official implementation of VGG19 with batch norm from Paszke et al. [2017]. As presented in Table 1, our method is consistently better than SNIP, with a larger gap as we increase sparsity. Surprisingly, GRASP achieves a slightly better performance than other methods at 95% sparsity, but collapses to random accuracy beyond that level.

Table 1: Test accuracies on Imagenet for different pruning methods and sparsities.

Sparsity percentage Accuracy	90%		95%		98%		99%	
	Top-1	Top-5	Top-1	Top-5	Top-1	Top-5	Top-1	Top-5
VGG19 (Baseline)	73.1	91.3						
SNIP Lee et al. [2019]	68.5	88.8	63.8	86.0	51.3	77.4	33.4	61.1
GRASP Wang et al. [2020]	69.5	89.2	67.6	87.8	0.1	0.5	0.1	0.5
FORCE (Ours)	69.8	89.5	65.9	86.9	53.9	79.1	40.4	67.8
Random	64.2	86.0	56.6	81.0	42.2	69.3	29.0	55.4

5.3 Analysis

Sparsity schedule To experimentally validate our approach (7), we conduct an ablation study where we compute the FORCE saliency after pruning (3) while varying the number of iterations T for different sparsity levels. In Figure 4 (a) we present the relative change in saliency between one-shot SNIP ($T = 1$) and FORCE ($T > 1$) with exponential mode (Eq (9)). In Appendix B.1 we also include results for linear mode (Eq (8)). As expected, for moderate levels of sparsity, using multiple iterations does not have a significant impact on the saliency. Nevertheless, as we target higher sparsity levels, we can see that the saliency can be better optimized when pruning iteratively.

As shown in Figures 2 and 3, for moderate sparsity levels, SNIP is comparable to FORCE, but as we move to higher sparsity levels the gap becomes larger. In Figure 4 (b) we fix sparsity at 99.5% and study the accuracy as we vary T . Each point is averaged over 3 trials. SNIP ($T = 1$) sub-networks are unable to train. As we move to iterative pruning, $T > 1$, accuracy increases and stabilizes. Note that the saliency follows a similar pattern as the accuracy, indicating a correlation between the two.

Complimentary to Figure 4 (a), in Appendix B.2 we analyse the evolution of FORCE and GRASP saliencies obtained by different pruning methods as we vary the sparsity. We observe FORCE is able to preserve both the FORCE saliency and the Gradient Norm better than the non-iterative methods for high sparsity levels *even though our saliency does not explicitly maximize the Gradient Norm*.

Extreme pruning and skip connections In Figure 2, we observe that FORCE is able to prune the Resnet50 network up to 99.99% sparsity without falling to random accuracy. In contrast, with VGG19 we could not prune more than 99.90% of the weights. In Appendix B.3 we visualize the structure of the networks after pruning. We observe that for Resnet50, all methods prune some layers completely. However, in the case of ResNets, even if a convolutional layer is entirely pruned, skip connections still allow the flow of forward and backward signal. On the other hand, architectures without skip connections, such as VGG, require non-empty layers to keep the flow of information. We hypothesize this is the reason why we are able to prune a Resnet network to higher sparsity levels than VGG.

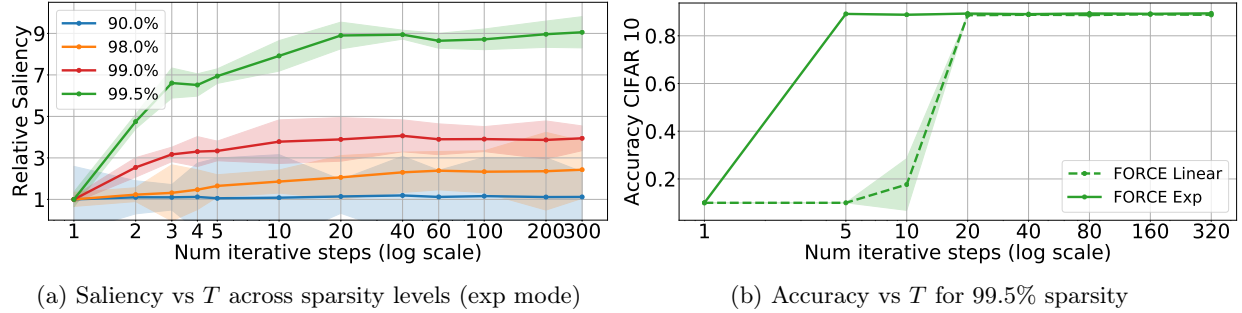


Figure 4: (a) FORCE saliency (6) obtained with our method normalized by saliency with one-shot SNIP, $T = 1$. Iterative pruning brings more gains for higher sparsity levels. (b) Test accuracy pruning with FORCE for different number of iterations T and modes.

5.4 Extreme Pruning of Resnet on Imagenet

In Table 2, we present the results for pruning a Resnet50 on Imagenet. Even though FORCE significantly outperforms other methods for extreme sparsity, it still is not able to obtain a practically useful performance. We hypothesize that, for a much more challenging task (Imagenet with 1000 classes), Resnet50 architecture might not be extremely overparametrized. For instance, VGG19 has 143.68M parameters while Resnet50 uses 25.56M (refer to Table 3). Thus, it might not be sensible to consider pruning Resnet50 for Imagenet at those sparsity levels and expect competitive results. On the other hand, the fact that random pruning can yield relatively trainable architectures for these sparsity levels is somewhat surprising and might indicate that there is still room for improvement in this direction. For instance, devising a criteria to know how much to prune, depending on the task and the function class at hand, would be of great use. We show these relatively negative results here to indicate potential future directions our community should emphasize on.

Table 2: Test accuracies on Imagenet for different pruning methods and sparsities.

Sparsity percentage	90%		95%		98%		99%	
	Top-1	Top-5	Top-1	Top-5	Top-1	Top-5	Top-1	Top-5
Resnet50 (Baseline)	75.6	92.8						
SNIP Lee et al. [2019]	61.5	83.9	44.3	69.6	7.0	17.2	0.1	0.5
GRASP Wang et al. [2020]	65.4	86.7	46.2	66.0	1.6	2.0	0.1	0.5
FORCE (Ours)	63.7	85.5	54.7	78.9	42.1	67.7	31.1	56.1
Random	64.6	86.0	57.2	80.8	45.0	70.4	32.4	57

6 Discussion

We present FORCE, a method to perform pruning at initialization. We experimentally validate that our approach preserves the saliency better than current pruning at initialization methods and achieves state-of-the-art performance. As a matter of fact, we show that current state-of-the-art methods for pruning at initialization fall below the performance of random pruning for high levels of sparsity and provide some intuitions as to why these approximations are no longer valid in this regime. Our analysis of pruning at initialization methods provided in this paper brings some insights and provide an efficient framework to study the problem of training sparse neural networks from scratch, particularly at high sparsity levels. Moreover, our results on Imagenet show that there is still room for improvement in our choice of saliencies.

Acknowledgements

This work was supported by the ERC grant ERC-2012-AdG 321162-HELIOS, EPSRC grant Seebibyte EP/M013774/1 and EPSRC/MURI grant EP/N019474/1. We would also like to acknowledge the Royal Academy of Engineering and FiveAI. Pau de Jorge was an academic visitor fully funded by NAVER LABS Europe.

References

- Jonathan Frankle and Michael Carbin. The lottery ticket hypothesis: Finding sparse, trainable neural networks. In *International Conference on Learning Representations*, 2019. URL <https://openreview.net/forum?id=rJl-b3RcF7>.
- Namhoon Lee, Thalaiyasingam Ajanthan, and Philip Torr. SNIP: SINGLE-SHOT NETWORK PRUNING BASED ON CONNECTION SENSITIVITY. In *International Conference on Learning Representations*, 2019. URL <https://openreview.net/forum?id=B1VZqjAcYX>.
- Michael C Mozer and Paul Smolensky. Skeletonization: A technique for trimming the fat from a network via relevance assessment. In *Advances in Neural Information Processing Systems*, 1989.
- Erich Elsen, Marat Dukhan, Trevor Gale, and Karen Simonyan. Fast sparse convnets. *arXiv preprint arXiv:1911.09723*, 2019.
- Chaoqi Wang, Guodong Zhang, and Roger Grosse. Picking winning tickets before training by preserving gradient flow. In *International Conference on Learning Representations*, 2020. URL <https://openreview.net/forum?id=SkgsACVKPH>.
- Yann LeCun, John S Denker, and Sara A Solla. Optimal brain damage. In *Advances in neural information processing systems*, pages 598–605, 1990.
- Babak Hassibi, David G Stork, and Gregory J Wolff. Optimal brain surgeon and general network pruning. In *IEEE international conference on neural networks*, pages 293–299. IEEE, 1993.
- Song Han, Jeff Pool, John Tran, and William Dally. Learning both weights and connections for efficient neural network. In *Advances in neural information processing systems*, pages 1135–1143, 2015.
- Pavlo Molchanov, Stephen Tyree, Tero Karras, Timo Aila, and Jan Kautz. Pruning convolutional neural networks for resource efficient inference. In *International Conference on Learning Representations*, 2017.
- Yiwen Guo, Anbang Yao, and Yurong Chen. Dynamic network surgery for efficient dnns. In *Advances in neural information processing systems*, pages 1379–1387, 2016.
- Yves Chauvin. A back-propagation algorithm with optimal use of hidden units. In *Advances in neural information processing systems*, pages 519–526, 1989.
- Miguel Á. Carreira-Perpiñán and Yerlan Idelbayev. “learning-compression” algorithms for neural net pruning. In *The IEEE Conference on Computer Vision and Pattern Recognition (CVPR)*, June 2018.
- Christos Louizos, Max Welling, and Diederik P. Kingma. Learning sparse neural networks through l0 regularization. In *International Conference on Learning Representations*, 2018. URL <https://openreview.net/forum?id=H1Y8hhg0b>.
- Guillaume Bellec, David Kappel, Wolfgang Maass, and Robert Legenstein. Deep rewiring: Training very sparse deep networks. In *International Conference on Learning Representations*, 2018. URL https://openreview.net/forum?id=BJ_wN01C-.

- Decebal Constantin Mocanu, Elena Mocanu, Peter Stone, Phuong H Nguyen, Madeleine Gibescu, and Antonio Liotta. Scalable training of artificial neural networks with adaptive sparse connectivity inspired by network science. *Nature communications*, 9(1):1–12, 2018.
- Hesham Mostafa and Xin Wang. Parameter efficient training of deep convolutional neural networks by dynamic sparse reparameterization, 2019. URL <https://openreview.net/forum?id=S1xBioR5KX>.
- Xiaoliang Dai, Hongxu Yin, and Niraj K Jha. Nest: A neural network synthesis tool based on a grow-and-prune paradigm. *IEEE Transactions on Computers*, 68(10):1487–1497, 2019.
- Tim Dettmers and Luke Zettlemoyer. Sparse networks from scratch: Faster training without losing performance, 2020. URL <https://openreview.net/forum?id=ByeSYa4KPS>.
- Tao Lin, Sebastian U. Stich, Luis Barba, Daniil Dmitriev, and Martin Jaggi. Dynamic model pruning with feedback. In *International Conference on Learning Representations*, 2020. URL <https://openreview.net/forum?id=SJem8lSFwB>.
- Aditya Kusupati, Vivek Ramanujan, Raghav Somani, Mitchell Wortsman, Prateek Jain, Sham M. Kakade, and Ali Farhadi. Soft threshold weight reparameterization for learnable sparsity. *ArXiv*, abs/2002.03231, 2020.
- Namhoon Lee, Thalaiyasingam Ajanthan, Stephen Gould, and Philip H. S. Torr. A signal propagation perspective for pruning neural networks at initialization. In *International Conference on Learning Representations*, 2020. URL <https://openreview.net/forum?id=HJeTo2VFwH>.
- Alex Krizhevsky et al. Learning multiple layers of features from tiny images, 2009.
- Olga Russakovsky, Jia Deng, Hao Su, Jonathan Krause, Sanjeev Satheesh, Sean Ma, Zhiheng Huang, Andrej Karpathy, Aditya Khosla, Michael Bernstein, Alexander C. Berg, and Li Fei-Fei. ImageNet Large Scale Visual Recognition Challenge. *International Journal of Computer Vision (IJCV)*, 115(3):211–252, 2015. doi: 10.1007/s11263-015-0816-y.
- Adam Paszke, Sam Gross, Soumith Chintala, Gregory Chanan, Edward Yang, Zachary DeVito, Zeming Lin, Alban Desmaison, Luca Antiga, and Adam Lerer. Automatic differentiation in pytorch, 2017.
- Kaiming He, Xiangyu Zhang, Shaoqing Ren, and Jian Sun. Delving deep into rectifiers: Surpassing human-level performance on imagenet classification. In *Proceedings of the IEEE international conference on computer vision*, pages 1026–1034, 2015.
- Soufiane Hayou, Jean-Francois Ton, Arnaud Doucet, and Yee Whye Teh. Pruning untrained neural networks: Principles and analysis, 2020.
- Zhuang Liu, Mingjie Sun, Tinghui Zhou, Gao Huang, and Trevor Darrell. Rethinking the value of network pruning. In *International Conference on Learning Representations*, 2018.

A Pruning implementation details

Networks are initialized using the Kaiming normal initialization (He et al. [2015]). For CIFAR datasets, we train Resnet50² and VGG19³ architectures during 350 epochs with a batch size of 128. We start with a learning rate of 0.1 and divide it by 10 at 150 and 250 epochs. As optimizer we use SGD with momentum 0.9 and weight decay 5×10^{-4} . We separate 10% of the training data for validation and report results on the test set. We perform mean and std normalization and augment the data with random crops and horizontal flips. For Tiny-Imagenet, we use the same architectures. We train during 300 epochs and divide the learning rate by 10 at 1/2 and 3/4 of the training. Other hyper-parameters remain the same. For ImageNet training, we adapt the official code⁴ of Paszke et al. [2017] and we use the default settings. In this case, we use the Resnet50 and VGG19 with batch normalization architectures as implemented in Paszke et al. [2017].

In the case of FORCE, we adapt the same public implementation⁵ of SNIP as Wang et al. [2020]. Instead of defining an auxiliary mask to compute the saliencies, we compute the product of the weight times the gradient, which was shown to be equivalent in Lee et al. [2020]. As for GRASP, we use their public code.⁶ For all pruning methods, we implement a pruned connection by setting the corresponding weight to 0 and forcing the gradient to be 0. This way, a pruned weight will remain 0 during training.

An important difference between SNIP and GRASP implementations is in the way they select the mini-batch to compute the saliency. SNIP implementation simply loads a batch from the dataloader. In contrast, in GRASP implementation they keep loading batches of data until they obtain exactly 10 examples of each class, discarding redundant samples. In order to compare the methods in equal conditions, we decided to use the way SNIP collects the data since it is simpler to implement and does not require extra memory. This might cause small discrepancies between our results and the ones reported in Wang et al. [2020].

Table 3: Percentage of weights per layer for each network and dataset.

Layer type	Conv	Fully connected	BatchNorm	Bias	Prunable	Total
CIFAR10						
Resnet50	99.69	0.09	0.11	0.11	99.78	23.52M
VGG19	99.92	0.03	0.03	0.03	99.95	20.04M
CIFAR100						
Resnet50	98.91	0.86	0.11	0.11	99.78	23.71M
VGG19	99.69	0.25	0.03	0.03	99.94	20.08M
TinyImagenet						
Resnet50	98.06	1.71	0.11	0.11	99.78	23.91M
VGG19	99.44	0.51	0.03	0.03	99.94	20.13M
Imagenet						
Resnet50	91.77	8.01	0.10	0.11	99.79	25.56M
VGG19	13.93	86.05	0.01	0.01	99.98	143.68M

A meaningful design choice regarding SNIP and GRASP implementations is that they only prune convolutional and fully connected layers. These layers constitute the vast majority of parameters in most networks, however, as we move to high sparsity regimes, batch norm layers constitute a non-negligible amount. For CIFAR10, batch norm plus biases constitute 0.2% and 0.05% of the parameters of Resnet50 and VGG19 networks respectively. For consistency, we have as well restricted pruning to convolutional and fully connected layers and reported percentage sparsity with respect to the prunable parameters, as is also done in Lee et al. [2019] and Wang et al. [2020] to the best of our knowledge. In Table 3 we show the percentage of prunable weights

²<https://github.com/kuangliu/pytorch-cifar/blob/master/models/resnet.py>

³<https://github.com/alecwangcq/GraSP/blob/master/models/base/vgg.py>

⁴<https://github.com/pytorch/examples/tree/master/imagenet>

⁵<https://github.com/mi-lad/snip>

⁶<https://github.com/alecwangcq/GraSP>

for each network and dataset we use. In future experiments we will explore the performance of pruning at initialization when including batch norm layers and biases as well.

B Further analysis of pruning at initialization

B.1 FORCE saliency vs T

In Figure 4 we have seen that as we increase the sparsity level, FORCE obtains a higher saliency as we increase the number of iterations. Moreover, we have seen that when using the exponential decay mode we need less iterations than when using linear mode to reach the same accuracy. In Figure 5 we compare the gain in saliencies as we increase the number of iterations between the linear and exponential decay modes. As expected, we see that for the linear mode we need a larger number of iterations to plateau. Interestingly, the saliency we are able to obtain when using a large number of iterations is comparable with both schedules. We hypothesize that when we use a large T , no matter the decay schedule, we always make small enough steps.

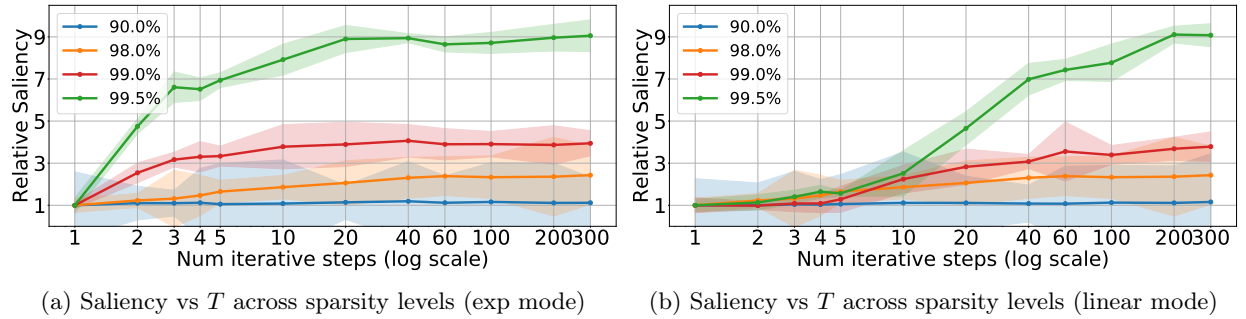


Figure 5: FORCE saliency (6) obtained with iterative pruning normalized by the saliency obtained with one-shot SNIP, $T = 1$. (a) Using exponential mode (b) Using linear mode. Note how both schedules eventually achieve similar saliencies, but we need a larger amount of iterations for the linear schedule. Each point is averaged over 5 trials.

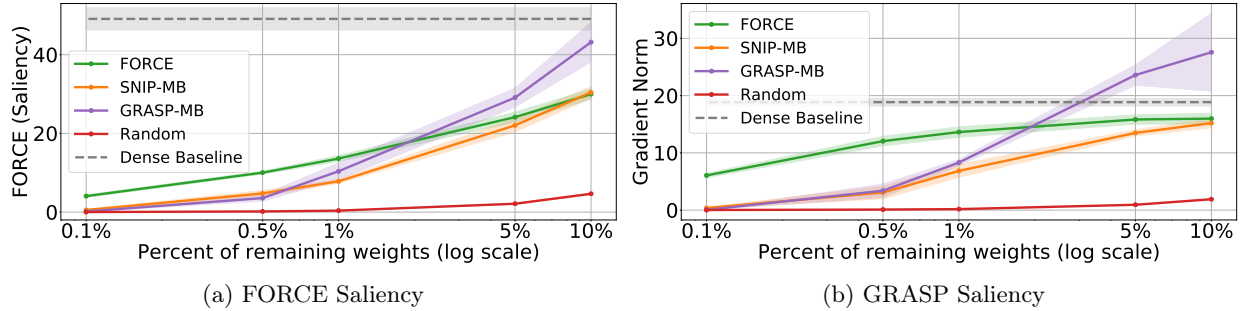


Figure 6: (a) FORCE saliency (6) averaged over 5 trials for different number of iterations T with exponential mode. (b) Gradient norm after pruning with different methods. Each point is the average of five trials. Note that with $T = 1$ FORCE is equivalent to one-shot SNIP.

B.2 Saliencies vs Sparsity

Complimentary to Figure 4 (a), we analyse the evolution of the FORCE and GRASP saliencies obtained by different pruning methods as we vary the pruning sparsity. In Figure 6 (a) we observe that both SNIP

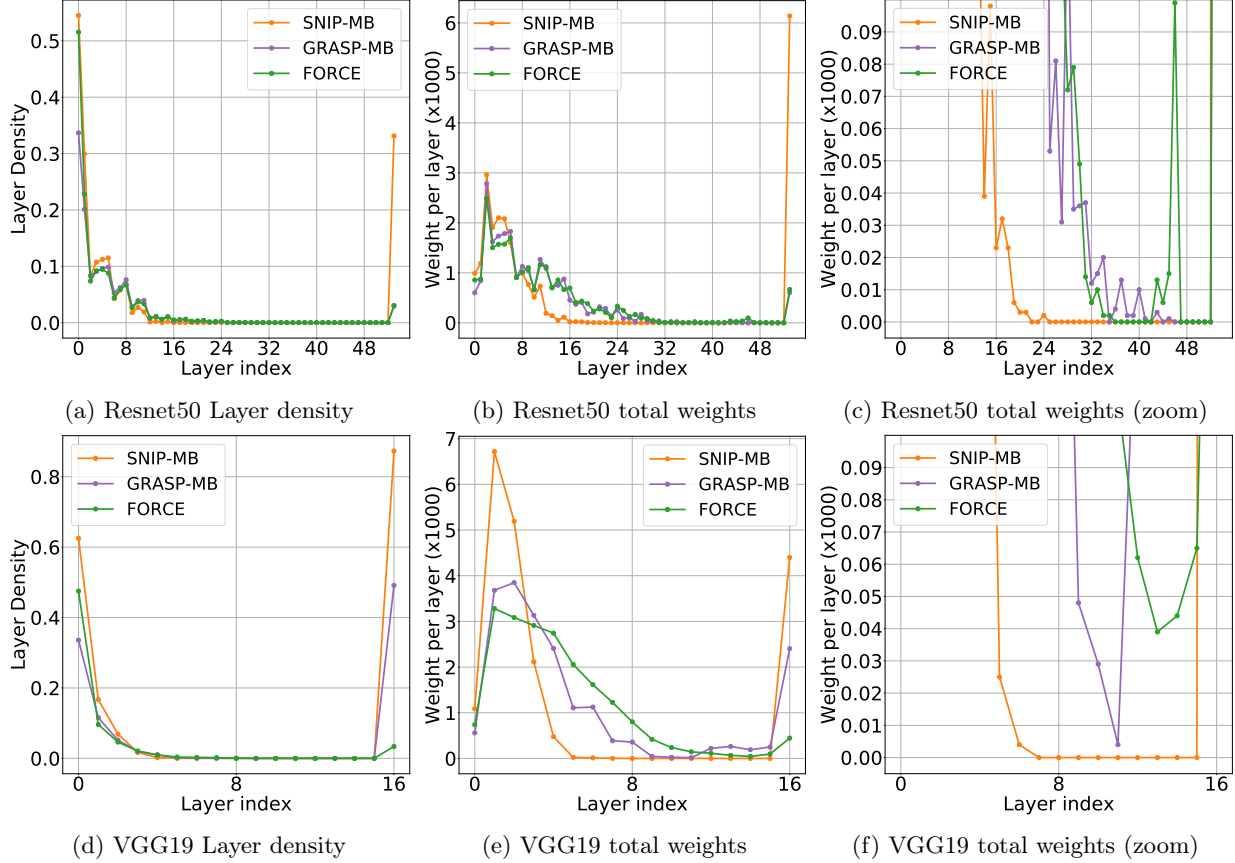


Figure 7: Visualization of remaining weights after pruning 99.9% of weight of Resnet-50 and VGG-19 for CIFAR-10. (a) and (d) show the fraction of remaining weights for each prunable layer. (b) and (e) show the actual number of remaining weights and (c) and (f) zoom to the bottom part of the plot. Observe in (c) and (f) that some layers have exactly 0 weights left, so they are removed entirely.

and GRASP tend to maximize the FORCE saliency, showing the two methods are related. As expected, we observe that the saliency decreases as we increase sparsity, but FORCE is able to preserve the saliency much better than the one-shot methods. In Figure 6 (b) we show a similar behaviour for the Gradient Norm after pruning. Particularly, we would like to stress that our method is preserving the Gradient Norm better than GRASP as we increase sparsity, even though we are not explicitly enforcing it.

B.3 Network structure after pruning

In Figure 7 we visualize the structure of the networks after pruning 99.9% of the parameters. We show the fraction of remaining weights and the total number of remaining weights per layer after pruning. As seen in (a) and (d), all analysed methods show a tendency to preserve the initial and final layers and to prune more heavily the deep convolutional layers, this is consistent with results reported in Wang et al. [2020]. In (b) and (e), FORCE has a structure closer to GRASP than SNIP. This is reasonable since, unlike SNIP, they are both optimizing the network after pruning. Nevertheless, in the zoomed plots (c) and (f) we observe how FORCE and GRASP are not so similar. Particularly, we would like to point out that FORCE preserves more weights on the deeper layers than GRASP and SNIP for VGG19 while it has seemingly the opposite behaviour for Resnet50. In the main text we discussed how skip connections can keep the flow of signal through the network even if we completely prune some convolutional layers. Interestingly, in (c) we observe

how FORCE has a larger amount of completely pruned layers than GRASP, however, there are a few deep layers with a significantly larger amount of unpruned weights. This seems to indicate that when extreme sparsity is required, it is more efficient to have fewer layers with more weights than several extremely sparse layers.

C Local optimal masks

Definition 1 ((p, ϵ) -local optimal mask). Consider any two sets⁷ $\mathbf{c}_t \subseteq \{1, \dots, m\}$ and $\mathbf{c}_{t+1} \subset \mathbf{c}_t$. For any $\epsilon > 0$ and $0 \leq p \leq |\mathbf{c}_t \setminus \mathbf{c}_{t+1}|$, \mathbf{c}_{t+1} is a (p, ϵ) local optimal with respect to \mathbf{c}_t if the following holds

$$S(\theta, \mathbf{c}_{t+1}) \geq S(\theta, (\mathbf{c}_{t+1} \setminus S_-) \cup S_+) - \epsilon \quad (10)$$

for all $S_- \subset \mathbf{c}_{t+1}, |S_-| = p$ and $S_+ \subset (\mathbf{c}_t \setminus \mathbf{c}_{t+1}), |S_+| = p$.

Definition 2 (CRS; Coordinate-Restricted-Smoothness). Given a function $\mathcal{L} : \mathbb{R}^m \rightarrow \mathbb{R}$ (which encodes both the network architecture and the dataset), \mathcal{L} is said to be λ_c -Coordinated Restricted Smooth with respect to $\mathbf{c} \subseteq \{1, \dots, m\}$ if there exists a real number λ_c such that

$$\|\mathbf{c} \odot \nabla \mathcal{L}(\mathbf{w} \odot \mathbf{c}) - \mathbf{c} \odot \nabla \mathcal{L}(\mathbf{w} \odot \hat{\mathbf{c}})\|_\infty \leq \lambda_c \|\mathbf{w} \odot \mathbf{c} - \mathbf{w} \odot \hat{\mathbf{c}}\|_1 \quad (11)$$

for all $\mathbf{w} \in \mathbb{R}^m$ and $\hat{\mathbf{c}} \subset \mathbf{c}$. When $s = |\mathbf{c} \setminus \hat{\mathbf{c}}|$, an application of Holder's inequality shows

$$\lambda_c \|\mathbf{w} \odot \mathbf{c} - \mathbf{w} \odot \hat{\mathbf{c}}\|_1 \leq \lambda_c \|\mathbf{w}\|_\infty \|\mathbf{c} - \hat{\mathbf{c}}\|_1 = \lambda_c s \|\mathbf{w}\|_\infty$$

We define \mathcal{L} to be Λ -total CRS if there exists a function $\Lambda : \{0, 1\}^m \rightarrow \mathbb{R}$ such that for all $\mathbf{c} \in \{0, 1\}^m$ \mathcal{L} is $\Lambda(\mathbf{c})$ -Coordinate-Restricted-Smooth with respect to \mathbf{c} (for ease of notation we use $\Lambda(\mathbf{c}) = \lambda_c$).

Theorem 1 (Informal). *The mask \mathbf{c}_{t+1} produced from \mathbf{c}_t by SNIP-It is $(p, 2\lambda_p \|\theta\|_\infty^2 |\mathbf{c}_t|)$ -local optimal if the \mathcal{L} is Λ -CRS.*

Proof. Consider the masks \mathbf{c}_t and \mathbf{c}_{t+1} where the latter is obtained by one step of SNIP-It on the former. Let S_- and S_+ be any set of size p such that $S_- \subset \mathbf{c}_{t+1}$ and $S_+ \subset (\mathbf{c}_t \setminus \mathbf{c}_{t+1})$. Finally, for ease of notation we define $\zeta = (\mathbf{c}_{t+1} \setminus S_-) \cup S_+$

$$\begin{aligned} S(\theta, \zeta) - S(\theta, \mathbf{c}_{t+1}) &= \sum_{i \in \zeta} |\theta_i \cdot \nabla \mathcal{L}(\theta \odot \zeta)_i| - \sum_{i \in \mathbf{c}_{t+1}} |\theta_i \cdot \nabla \mathcal{L}(\theta \odot \mathbf{c}_{t+1})_i| \\ &= \underbrace{\sum_{i \in \mathbf{c}_{t+1}} |\theta_i \cdot \nabla \mathcal{L}(\theta \odot \zeta)_i| - \sum_{i \in \mathbf{c}_{t+1}} |\theta_i \cdot \nabla \mathcal{L}(\theta \odot \mathbf{c}_{t+1})_i|}_{\Gamma_1} \\ &\quad + \underbrace{\sum_{i \in S_+} |\theta_i \cdot \nabla \mathcal{L}(\theta \odot \zeta)_i|}_{\Gamma_2} - \underbrace{\sum_{i \in S_-} |\theta_i \cdot \nabla \mathcal{L}(\theta \odot \zeta)_i|}_{\Gamma_3} \end{aligned} \quad (12)$$

Let us look at the three terms individually. We assume that \mathcal{L} is Λ -CRS.

$$\begin{aligned} \Gamma_1 &= \sum_{i \in \mathbf{c}_{t+1}} |\theta_i \cdot \nabla \mathcal{L}(\theta \odot \zeta)_i| - |\theta_i \cdot \nabla \mathcal{L}(\theta \odot \mathbf{c}_{t+1})_i| \\ &\leq \|\mathbf{c}_{t+1} \odot \theta \odot \nabla \mathcal{L}(\theta \odot \mathbf{c}_{t+1}) - \mathbf{c}_{t+1} \odot \theta \odot \nabla \mathcal{L}(\theta \odot \zeta)\|_1 && \text{By Triangle Inequality} \\ &\leq \|\mathbf{c}_{t+1} \odot \theta\|_1 \|\mathbf{c}_{t+1} \odot \nabla \mathcal{L}(\theta \odot \mathbf{c}_{t+1}) - \mathbf{c}_{t+1} \odot \nabla \mathcal{L}(\theta \odot \zeta)\|_\infty && \text{By Holder's Inequality} \\ &\leq 2\lambda_{\mathbf{c}_{t+1}} |\mathbf{c}_{t+1}| p \|\theta\|_\infty^2 && \because \mathcal{L} \text{ is } \Lambda\text{-CRS} \end{aligned} \quad (13)$$

⁷For ease of notation, we will use this representation interchangeably with its binary encoding i.e. a m -dimensional binary vector with its support equal to \mathbf{c}

$$\begin{aligned}
\Gamma_2 &= \sum_{i \in S_+} |\theta_i \cdot \nabla \mathcal{L}(\theta \odot \zeta)_i| - |\theta_i \cdot \nabla \mathcal{L}(\theta \odot \mathbf{c}_t)_i| + |\theta_i \cdot \nabla \mathcal{L}(\theta \odot \mathbf{c}_t)_i| \\
&\leq \sum_{i \in S_+} |\theta_i \cdot \nabla \mathcal{L}(\theta \odot \mathbf{c}_t)_i| + \lambda_{\mathbf{c}_t} p \|\theta\|_\infty^2 (|\mathbf{c}_t| - |\mathbf{c}_{t+1}|) \quad \because |\mathbf{c}_t \setminus \zeta| = |\mathbf{c}_t| - |\mathbf{c}_{t+1}|, \quad (14)
\end{aligned}$$

$$\begin{aligned}
\Gamma_3 &= - \sum_{i \in S_-} |\theta_i \cdot \nabla \mathcal{L}(\theta \odot \zeta)_i| + |\theta_i \cdot \nabla \mathcal{L}(\theta \odot \mathbf{c}_t)_i| - |\theta_i \cdot \nabla \mathcal{L}(\theta \odot \mathbf{c}_t)_i| \\
&\leq - \sum_{i \in S_-} |\theta_i \cdot \nabla \mathcal{L}(\theta \odot \mathbf{c}_t)_i| + \lambda_{\mathbf{c}_t} p \|\theta\|_\infty^2 (|\mathbf{c}_t| - |\mathbf{c}_{t+1}|), \quad (15)
\end{aligned}$$

Adding eqs. (14) and (15), we get

$$\begin{aligned}
\Gamma_2 + \Gamma_3 &\leq \sum_{i \in S_+} |\theta_i \cdot \nabla \mathcal{L}(\theta \odot \mathbf{c}_t)_i| - \sum_{i \in S_-} |\theta_i \cdot \nabla \mathcal{L}(\theta \odot \mathbf{c}_t)_i| + 2\lambda_{\mathbf{c}_t} p \|\theta\|_\infty^2 (|\mathbf{c}_t| - |\mathbf{c}_{t+1}|) \\
&\leq 2\lambda_{\mathbf{c}_t} p \|\theta\|_\infty^2 (|\mathbf{c}_t| - |\mathbf{c}_{t+1}|) - \gamma p \quad (16)
\end{aligned}$$

where $\gamma = \min_{i \in \mathbf{c}_{t+1}, j \in (\mathbf{c}_t \setminus \mathbf{c}_{t+1})} |\theta_i \nabla \mathcal{L}(\theta \odot \mathbf{c}_t)_i| - |\theta_j \nabla \mathcal{L}(\theta \odot \mathbf{c}_t)_j| \geq 0$

Substituting eqs. (13) and (16) into (12) we get

$$\begin{aligned}
S(\theta, \zeta) - S(\theta, \mathbf{c}_{t+1}) &\leq 2\lambda_{\mathbf{c}_{t+1}} |\mathbf{c}_{t+1}| p \|\theta\|_\infty^2 + 2\lambda_{\mathbf{c}_t} p \|\theta\|_\infty^2 (|\mathbf{c}_t| - |\mathbf{c}_{t+1}|) - \gamma p \\
&= 2\lambda_{\mathbf{c}_{t+1}} p \|\theta\|_\infty^2 (|\mathbf{c}_{t+1}| + (|\mathbf{c}_t| - |\mathbf{c}_{t+1}|)) - \gamma p \\
S(\theta, \mathbf{c}_{t+1}) &\geq S(\theta, \zeta) - 2\lambda_{\mathbf{c}_{t+1}} p \|\theta\|_\infty^2 |\mathbf{c}_t| + \gamma p \\
S(\theta, \mathbf{c}_{t+1}) &\geq S(\theta, \zeta) - 2\lambda_{\mathbf{c}_{t+1}} p \|\theta\|_\infty^2 |\mathbf{c}_t|
\end{aligned}$$

□

D Stable Resnet

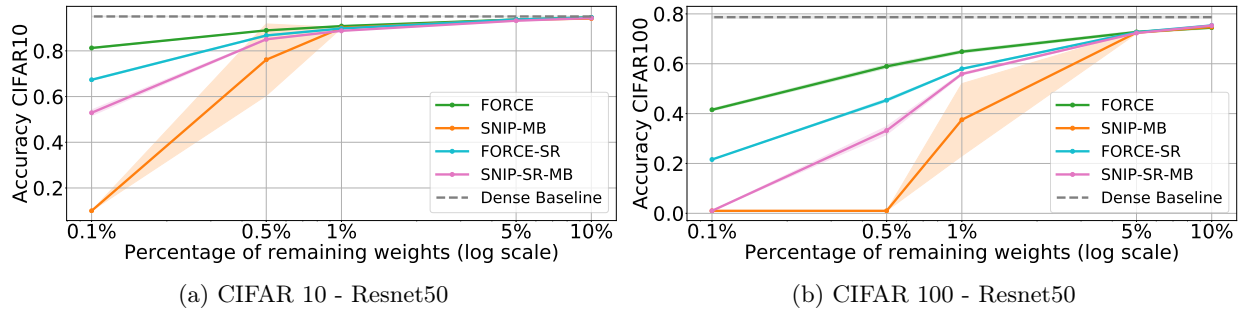


Figure 8: Test accuracies on CIFAR-10/100 for different pruning methods. Each point is the average over 3 runs of prune-train-test. The shaded areas denote the standard deviation of the runs (sometimes too small to be visualized).

In Hayou et al. [2020], the authors present a theoretical analysis of pruning at initialization. In their analysis, they show that residual networks are always well-conditioned for pruning with SNIP and present a scaling of residual blocks that makes Resnets more stable to prune at high sparsity levels. We implemented their Stable Resnet and performed an ablation study to check if we observe any gain with respect to the standard

Resnet implementation. In Figure 8 we present the test accuracies for CIFAR-10/100. As observed in Hayou et al. [2020], when we prune Stable Resnet with SNIP, denoted with an additional (-SR), we observe an improvement with respect to regular Resnet. Interestingly, when we prune a Stable Resnet with FORCE we see a drop in performance. In Hayou et al. [2020], they present experiments where they use Stable Resnet with GRASP and they observe a slight decrease in performance. They state this is because their analysis is only valid for SNIP. Similarly, we hypothesize their analysis is not valid for our presented method which maximizes the connection sensitivity *after* pruning and skeletonizes the network progressively.

E Iterative pruning to maximize the gradient norm

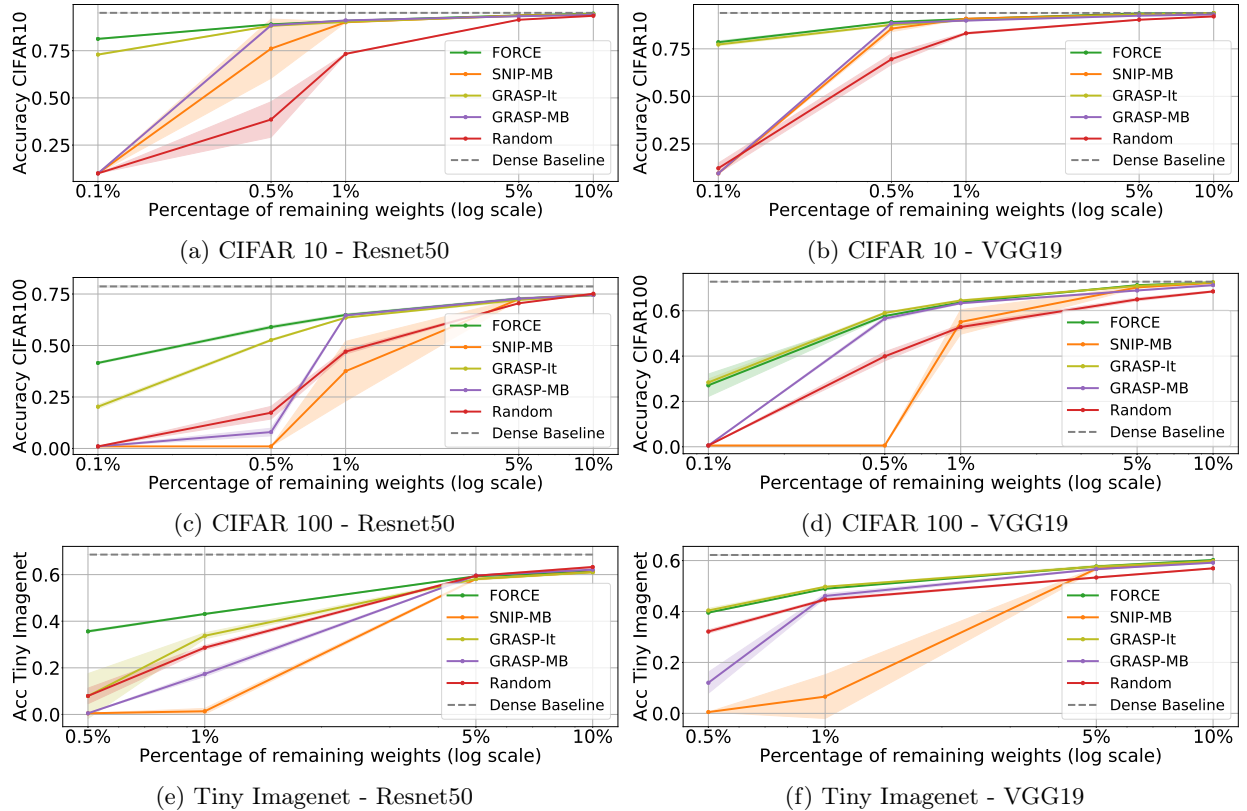


Figure 9: Test accuracies for different datasets and networks when pruned with different methods. Each point is the average over 3 runs of prune-train-test. The shaded areas denote the standard deviation of the runs (sometimes too small to be visible).

E.1 Maximizing the gradient norm using the gradient approximation

In order to maximize the gradient norm after pruning, the authors in Wang et al. [2020] use the first order Taylor’s approximation. While this seems to be better suited than SNIP for higher levels of sparsity, it assumes that pruning is a small perturbation on the weight matrix. We argue that this approximation will not be valid as we push towards extreme sparsity values. Our *gradient approximation* (refer to Section 4) can also be applied to maximize the gradient norm after pruning. In this case, we have

$$G(\theta, c) := \Delta \mathcal{L}(\theta \odot c) - \Delta \mathcal{L}(\theta) \approx \sum_{\{i: c_i=0\}} -[\nabla \mathcal{L}(\theta)_i]^2, \quad (17)$$

since pruned connections should have null gradients (as they will not be propagating backward signal through the network) and we assume gradients remain unchanged for unpruned weights (gradient approximation). Combining this approximation with Eq. (7), we obtain a new pruning method we name GRASP-It. Unlike FORCE, GRASP-It does not recover GRASP when $T = 1$.

In Figure 9 we compare GRASP-It to other pruning methods. We use the same settings as described in Section 5. We observe that GRASP-It outperforms GRASP in the extreme sparsity region. Moreover, for VGG19 architecture GRASP-It achieves comparable performance to FORCE. Nevertheless, for Resnet50 we see that GRASP-It performance falls below that of FORCE as we prune more weights.

Table 4: Test accuracies on Imagenet for different pruning methods and sparsities.

Sparsity percentage	90%		95%		98%		99%	
Accuracy	Top-1	Top-5	Top-1	Top-5	Top-1	Top-5	Top-1	Top-5
VGG19 (Baseline)	73.1	91.3						
SNIP Lee et al. [2019]	68.5	88.8	63.8	86.0	51.3	77.4	33.4	61.1
GRASP Wang et al. [2020]	69.5	89.2	67.6	87.8	0.1	0.5	0.1	0.5
FORCE	69.8	89.5	65.9	86.9	53.9	79.1	40.4	67.8
GRASP-It	68.5	88.7	62.6	84.7	47.2	73.3	29.1	52.7
Random	64.2	86.0	56.6	81.0	42.2	69.3	29.0	55.4
Resnet50 (Baseline)	75.6	92.8						
SNIP Lee et al. [2019]	61.5	83.9	44.3	69.6	7.0	17.2	0.1	0.5
GRASP Wang et al. [2020]	65.4	86.7	46.2	66.0	1.6	2.0	0.1	0.5
FORCE	63.7	85.5	54.7	78.9	42.1	67.7	31.1	56.1
GRASP-It	61.9	83.9	49.6	74.1	31.0	55.0	19.6	39.8
Random	64.6	86.0	57.2	80.8	45.0	70.4	32.4	57

In Table 4 we present the results of all pruning methods, including GRASP-It, when pruning VGG19 and Resnet50 for Imagenet. In this case, GRASP-It does not match GRASP for moderate sparsity levels, recall that GRASP-It does not recover GRASP when we only use one iteration, $T = 1$. However, as we increase the sparsity, we observe that GRASP quickly falls to random accuracy, while GRASP-It is able to yield a trainable network. Nevertheless, in all cases GRASP-It is surpassed or at least matched by FORCE.

E.2 Iterative GRASP (Pruning consistency)

We would like to note that the iterative method described in Eq. (7) is independent of the particular saliency and approximations we use. Therefore, it is natural to question what would be the result of pruning iteratively using the Taylor’s approximation presented in Wang et al. [2020] (4). Unfortunately, we found that all resulting masks yield networks unable to train. In light of this result, we performed some analysis of the behaviour of GRASP compared to that of SNIP and, in the following, we provide some insights as to why we can not use GRASP’s approximation iteratively.

In Liu et al. [2018], the authors show that applying a pruning method to the same architecture with different random initializations would yield consistent pruning masks. Specifically, they find that the percentage of pruned weights in each layer had very low variance. We reproduce the same experiment and additionally explore another dimension, the (global) sparsity level. Given an architecture, we prune it at varying levels of sparsity and extract the percentage of remaining weights at each layer. For each level of sparsity, we average the results over 3 trials of initialize-prune. As shown in Figure 2, both SNIP and GRASP have very low variance across initializations, on the other hand, as we vary the global sparsity with GRASP, the percentage of remaining weights for each layer is inconsistent. The layers that are most preserved at high levels of sparsity, such as the initial and last layers, are the most heavily pruned at low sparsity levels. The authors in Liu et al. [2018], reason that manually designed networks have layers which are more redundant than others. Therefore, pruning methods even this redundancies by pruning layers with different percentages.

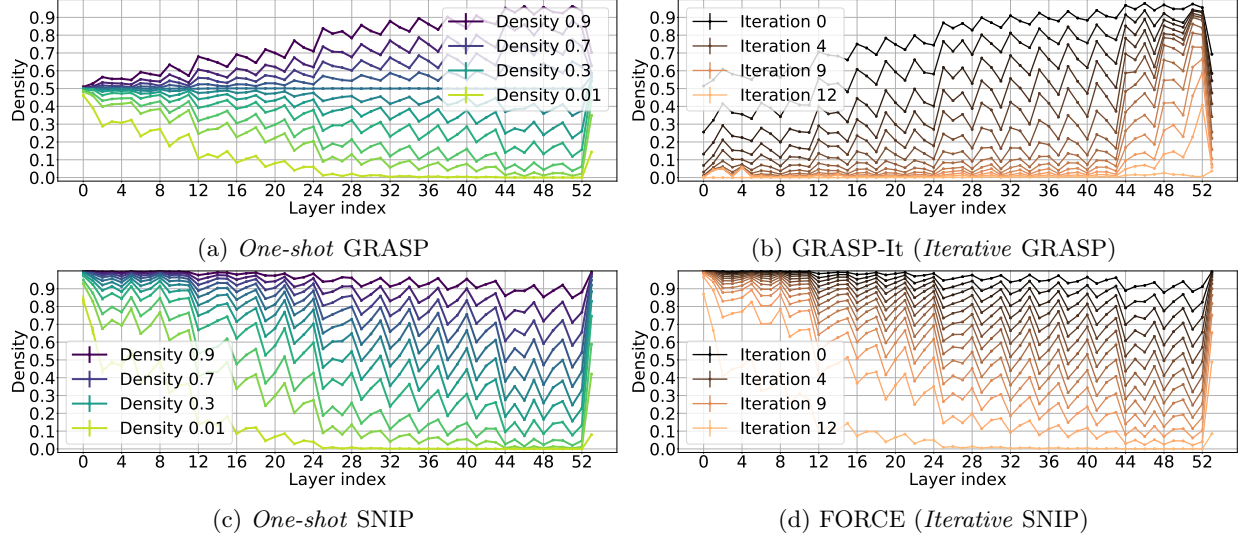


Figure 10: (a) - (c) Portion of remaining weights for each layer. Each point is an average of 3 runs and the error bars (hardly visible) denote standard deviation. (b) - (d) Portion of remaining weights for each intermediate mask that is computed during iterative pruning with global portion of remaining weights of 0.01.

We extend this reasoning, and hypothesize that pruning algorithms should always have preference for pruning the same (redundant) layers across all levels of sparsity. We denote this as *pruning consistency*. We observe that when applying iterative pruning to GRASP, the resulting masks tend to prune almost all of the weights at the initial and final layers, producing networks that are unable to converge. When using iterative pruning (7), we prune a small portion of remaining weights at each step. Thus, we are always in the low sparsity regime, where the GRASP behaviour is reversed. Conversely, when we use SNIP the behaviour changes completely. In this case, the preserved layers are consistent across sparsity levels, and when we use iterative pruning we obtain networks that reach high accuracy values.